JCTC Journal of Chemical Theory and Computation

Article

pubs.acs.org/JCTC

Energy Decomposition Analysis with a Stable Charge-Transfer Term for Interpreting Intermolecular Interactions

Ka Un Lao and John M. Herbert*

Department of Chemistry and Biochemistry, The Ohio State University, Columbus, Ohio 43210, United States

Supporting Information

ABSTRACT: Many schemes for decomposing quantum-chemical calculations of intermolecular interaction energies into physically meaningful components can be found in the literature, but the definition of the charge-transfer (CT) contribution has proven particularly vexing to define in a satisfactory way and typically depends strongly on the choice of basis set. This is problematic, especially in cases of dative bonding and for open-shell complexes involving cation radicals, for which one might expect significant CT. Here, we analyze CT interactions predicted by several popular energy decomposition analyses and ultimately recommend the definition afforded by constrained density functional theory (cDFT), as it is scarcely dependent on basis set and provides results that are in accord with chemical intuition in simple cases, and in quantitative agreement with experimental estimates of the CT energy, where available. For open-shell complexes, the cDFT approach affords CT energies that are in line with trends expected based on ionization potentials and electron affinities whereas some other definitions afford unreasonably large CT energies in large-gap systems, which are sometimes artificially offset by underestimation of van der Waals interactions by density functional theory. Our recommended energy decomposition analysis is a composite approach, in which cDFT is used to define the CT component of the interaction energy and symmetry-adapted perturbation theory (SAPT) defines the electrostatic, polarization, Pauli repulsion, and van der Waals contributions. SAPT/cDFT provides a stable and physically motivated energy decomposition that, when combined with a new implementation of open-shell SAPT, can be applied to supramolecular complexes involving molecules, ions, and/or radicals.

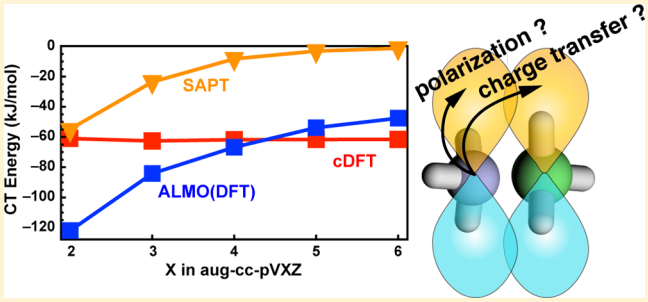

I. INTRODUCTION

As compared to closed-shell complexes, noncovalent interactions are less well understood in molecule−radical and radical−radical complexes, and in open-shell cases one might expect charge-transfer (CT) effects to be significant. Open-shell hydrogen bonds in radical complexes regulate electron-transfer processes in many enzymes,[1] wherein the half-filled orbital acts as a hydrogen-atom acceptor, forming a single-electron hydrogen bond.[2] Stabilization of this bond is thought to depend significantly upon electron transfer from the half-filled orbital into the σ^* orbital of the H-bond donor,[3] and the strength of the single-electron H-bond can be controlled *via* substituents added to either the donor or the acceptor. Protonation of the donor, *e.g.*, $H_3C^{\bullet}\cdots H_3O^+$ rather than $H_3C^{\bullet}\cdots H_2O$, can significantly increase single-electron H-bond strength. This can be explained in terms of the reduced distance between donor and acceptor as well as a lowering of the σ^* energy, both of which make H-bonding CT interactions more favorable.[4] Variations in the strength of molecule−radical interactions can significantly influence both the rate and outcome of chemical reactions,[5] *e.g.*, by reducing the reactivity of the radical, resulting in high product selectivity[6] for enantioselective organocatalysis.[7,8]

Despite the presumed importance of CT interactions in noncovalent complexes, direct experimental measurements of the magnitude of the CT contribution to the interaction energy are scarce. For closed-shell, binary gas-phase complexes involving H_2O, there are a few high-resolution molecular-beam scattering experiments that, in conjunction with charge-displacement analysis[9] and back-corrected intermolecular interaction potentials, have been used to obtain experimental values for the absolute magnitude of the CT interaction energy.[10−12] CT energies extracted from these experiments are approximately proportional to the amount of charge that is transferred, averaged over all orientations of the two monomers,[10−12] which is seen also in some theoretical analyses.[13,14] Stereospecific CT energies are very difficult to estimate from experiment;[10−12] thus a reliable CT interaction energy from theoretical calculations would be quite useful, but this has proven problematic.

Good electronic structure calculations can provide accurate values for the *total* noncovalent interaction energy between small- to medium-sized molecules, or between fragments of larger molecules.[15−19] What is often desired, however, is a

Received: February 11, 2016
Published: April 6, 2016

DOI: 10.1021/acs.jctc.6b00155
J. Chem. Theory Comput. 2016, 12, 2569−2582

partition of the interaction energy into physically meaningful components, such as electrostatic interactions, Pauli (or "exchange") repulsion, induction (also know as polarization), dispersion (the London or van der Waals interaction), and CT. Such a partition may aid in predicting how a certain chemical modification will alter the interaction energy, but unfortunately any such partition comes with some degree of arbitrariness. This has given rise to quite a number of energy decomposition analysis (EDA) methods;[13,20−35] see refs 36 and 37 for recent reviews.

This work is focused specifically on intermolecular interactions, and for such cases an EDA that we find particularly attractive is symmetry-adapted perturbation theory (SAPT).[38−41] This approach computes the interaction energy ΔE_{AB} of the A···B dimer system directly, *via* perturbation theory, rather than by energy difference ($\Delta E_{AB} = E_{AB} - E_A - E_B$), and is therefore free of the artifactual basis-set superposition error (BSSE) that ordinarily leads to dramatic overestimation of ΔE_{AB} except when very large basis sets (or counterpoise correction) are employed.[42−44] The structure of the perturbation series provides a natural decomposition of the interaction energy into electrostatic, exchange (or Pauli) repulsion, induction, and dispersion energy components, each with a well-defined basis-set limit,[39] and SAPT-EDA is increasingly being used as a means to parametrize physically motivated classical force fields.[45,46]

Unfortunately, the CT contribution is not separated in this decomposition but rather is subsumed within the induction term, for reasons that are illustrated schematically in Figure 1. When the basis set is small, there is a clear distinction between excitations (perturbations) that represent polarization originating in the presence of the other monomer, versus those that should be categorized as intermonomer CT, but this distinction disappears as the unoccupied orbitals centered on one monomer begin to overlap significantly with those centered on the other monomer. For this reason, attempts to isolate the CT energy in SAPT tend to be strongly basis-set dependent,[39,47] and it can be argued that within this framework the CT energy should vanish in the limit of a complete basis set.[47] Attempts to define the CT energy with various other EDAs that are based on self-consistent field (SCF) calculations face similar difficulties,[29,48] since molecular orbitals (MOs) on one monomer will inevitably spread to the other as the quality of the basis set improves. Although all of the calculations reported here employ atom-centered Gaussian basis functions, note that the ambiguity outlined in Figure 1 is a problem with *molecular* (rather than atomic) orbitals, and thus persists in plane-wave or even grid-based SCF calculations.

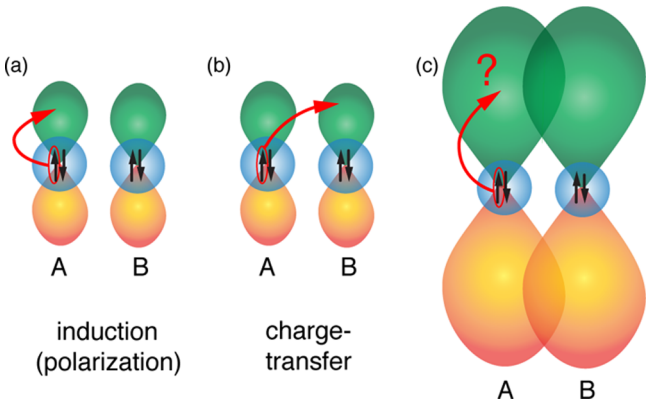

Figure 1. Schematic illustration of why the distinction between the CT and induction energies in SAPT depends strongly on basis set. In panels a and b, the basis set is small and therefore most orbitals are relatively localized around one monomer or the other. (a) An excitation from an occupied MO (in blue) that is centered on monomer A to a virtual MO (in green and orange) that is also centered on A either creates or enhances a dipole moment on monomer A, whose formation is driven by the perturbing influence of monomer B. This is the epitome of induction. (b) A CT interaction, in contrast, involves excitation from an occupied MO on monomer A to a virtual orbital associated with monomer B (as shown here), or *vice versa*. (c) In a larger basis set, where the virtual orbitals on one monomer extend into close proximity with the virtual orbitals on the other monomer, the distinction between induction and CT excitations becomes ambiguous, as it could be argued that even the nominally induction-type excitation depicted in panel c possesses some CT character.

For these reasons, there is need for a simple and reliable EDA for intermolecular interactions that includes a well-defined CT contribution, as an interpretative tool for noncovalent chemistry. Ideally, such an EDA should afford CT energies that correlate with chemical intuition in obvious cases. For example, the CT energy should decrease as a function of intermolecular separation. As suggested and demonstrated in previous computational studies of alkyl and aryl radicals,[49] CT energies should correlate linearly with $(IE - EA)^{-1}$, where IE is the ionization energy of the donor species and EA is the electron affinity of the acceptor. Finally, the CT energy should not depend strongly on the choice of basis set, at least for medium- to high-quality basis sets.

Constrained DFT[50] (cDFT) has recently been suggested as a means to sidestep the strong basis-set dependence inherent to most orbital-based definitions of CT.[51,52] In this approach, one computes a "CT-free" reference electron density by carrying out a variational DFT calculation on a supramolecular complex but with a constraint that requires each monomer density integrate to an integer number of electrons. The difference between the cDFT energy and that of an unconstrained DFT calculation affords a means to quantify the energy-lowering associated with electron flow upon assemblage of the complex from its constituent monomers.[51,52] This definition of CT depends on densities but not orbitals and is therefore only weakly dependent on the choice of basis set.[52]

In the present work, we combine this cDFT-based definition of CT with SAPT-EDA for the remaining energy components, using a new, open-shell implementation of SAPT.[53] As noted above, some or all of the CT energy in SAPT-EDA (tending toward "all" in the complete-basis limit) is contained in the term that is nominally labeled "induction". We use cDFT to separate out the CT energy, leaving the rest as the "true" induction energy. We will demonstrate that the combined SAPT/cDFT-EDA has several chemically desirable features. It reproduces the anticipated trend down the group I alkali cations for both $M^+\cdots H_2O$ and $M^+\cdots C_6H_6$ complexes; affords good correlation between the CT energy and the inverse gap, $(IE - EA)^{-1}$, in open-shell complexes; and is in reasonable agreement with CT energies extracted from molecular-beam experiments, in a few cases where such data are available. In addition, the use of SAPT allows for a well-defined separation of the dispersion energy from the other energy components, whereas this separation is more problematic in DFT-based EDAs. (This separability is also useful in SAPT, since second-order dispersion is notoriously inaccurate but can be replaced

DOI: 10.1021/acs.jctc.6b00155
J. Chem. Theory Comput. 2016, 12, 2569−2582

by improved treatments of this term alone.[19,40,41,54,55]) Most notably, the CT energy in SAPT/cDFT-EDA is only weakly dependent on basis set, which cannot be said for most orbital-based EDAs, including SAPT without the additional cDFT step. Finally, the orbital-based SAPT parts of our proposed EDA are free of BSSE without the need for counterpoise correction. As such, we consider that this approach affords meaningful and robust definitions for all of the various components of the intermolecular interaction energy and thus may be very useful for providing a theoretical basis for the "chemical intuition" of noncovalent interactions.

II. THEORY

IIA. ALMO-EDA. A popular form of EDA in recent years is one developed originally by Mo, Gao, and co-workers,[26,27] who called it the "block-localized wave function EDA" (BLW-EDA), and which is equivalent to the "absolutely-localized MO" (ALMO) version of EDA that has been further developed and popularized by Head-Gordon and co-workers.[13,29,30,56,57] We use the term ALMO-EDA here, where "ALMO" indicates that the MOs on a given monomer are constrained to be formed from linear combinations of Gaussian basis functions centered on the same monomer, hence "absolutely localized". This offers certain advantages relative to some other EDAs, as it allows for a fully self-consistent and variational treatment of polarization, with a well-defined separation between polarization and CT. Although versions of ALMO-EDA based on correlated wave functions have been developed recently,[58,59] we confine ourselves to the DFT-based version, which is the most well-established and the most affordable.

Both BLW-EDA and the original version of ALMO-EDA exhibit strong basis-set dependence in both the polarization and CT components of the interaction energy,[48,56] as will be documented here. Very recently, "fragment electric field response functions" (FERFs) have been introduced as a novel fragment-blocked basis that attempts to overcome sensitivity to basis set. Initial results suggest that the use of FERFs permits stable (and nontrivial) basis-set limits for the polarization and CT energies, with the use of dipole and quadrupole functions being recommended,[56] though this choice is not unique. In this work, we employ the original version of ALMO-EDA.[29]

The interaction energy in ALMO-EDA is partitioned according to[29]

$$\Delta E^{\mathrm{ALMO}} = \Delta E^{\mathrm{ALMO}}_{\mathrm{FRZ}} + \Delta E^{\mathrm{ALMO}}_{\mathrm{POL}} + \Delta E^{\mathrm{ALMO}}_{\mathrm{CT}} \tag{1}$$

where the components are the "frozen-density" energy, the polarization energy, and the CT energy, respectively. (For simplicity, the energy associated with geometric distortion of the monomers is omitted in this work.) The $\Delta E^{\mathrm{ALMO}}_{\mathrm{FRZ}}$ term includes electrostatics, dispersion, and Pauli repulsion. It is based on an antisymmetric product of monomer wave functions (the Heitler–London wave function) that is *not* variationally optimized, as that optimization would amount to polarization. The polarization term is computed as the energy difference between the frozen-density state and the variationally optimized intermediate state (Ψ_{ALMO}), using the "SCF for molecular interactions" (SCF-MI) procedure.[60] Finally. the CT term in eq 1 is defined as[29]

$$\Delta E^{\mathrm{ALMO}}_{\mathrm{CT}} = E[\Psi] - E[\Psi_{\mathrm{ALMO}}] + \Delta E^{\mathrm{BSSE}} \tag{2}$$

where Ψ is the fully optimized SCF wave function for the dimer and ΔE^{BSSE} is the counterpoise correction.[42]

It has recently been suggested how the electrostatic, dispersion, and Pauli repulsion energies might be separated within the $\Delta E^{\mathrm{ALMO}}_{\mathrm{FRZ}}$ term.[30] Although the primary focus of this work is the CT energy, the dispersion interaction is also very different within ALMO-EDA as compared to our proposed SAPT/cDFT-EDA, and thus warrants some comment. The definition of the dispersion energy in a DFT calculation is problematic for several reasons, not least of which is that method's historical difficulty in the description of weak, long-range interactions. Although empirical dispersion corrections ("DFT+D") go a long way toward rectifying this problem,[61] the "+D" part of a DFT+D calculation should not be considered to be the dispersion energy *per se*,[62] as there is inevitably some double counting of electron correlation in the middle-distance regime.[61,62]

The definition of dispersion suggested in ref 30, which is valid for both DFT+D as well as for modern, nonlocal functionals that treat dispersion in a less *ad hoc* way, is

$$E_{\mathrm{disp}} = E_{\mathrm{xc}}[\mathbf{P}_{\mathrm{init}}] - E_{\mathrm{xc}}[\mathbf{P}_{\mathrm{A}}] - E_{\mathrm{xc}}[\mathbf{P}_{\mathrm{B}}] - (E^{\mathrm{DF}}_{\mathrm{xc}}[\mathbf{P}_{\mathrm{init}}] - E^{\mathrm{DF}}_{\mathrm{xc}}[\mathbf{P}_{\mathrm{A}}] - E^{\mathrm{DF}}_{\mathrm{xc}}[\mathbf{P}_{\mathrm{B}}]) \tag{3}$$

where $\mathbf{P}_{\mathrm{init}}$ is the density matrix corresponding to the antisymmetric product of monomer wave functions and $\mathbf{P}_{\mathrm{A}}$ and $\mathbf{P}_{\mathrm{B}}$ are orthogonal projection operators such that $\mathbf{P}_{\mathrm{A}} \oplus \mathbf{P}_{\mathrm{B}}$ projects onto the same space as $\mathbf{P}_{\mathrm{init}}$. The functional E_{xc} is whatever exchange–correlation functional is used to compute the interaction energy, whereas $E^{\mathrm{DF}}_{\mathrm{xc}}$ is a "dispersion-free" functional. For the latter, one could envision using the "dispersionless density functional" (dlDF) of Szalewicz and co-workers,[63] in which the M05-2X functional was reparametrized using a data set from which SAPT(DFT)[40,41] dispersion energies were first removed, but in ref 30 the dispersion-free functional is taken to be Hartree–Fock (HF) theory.

IIB. SAPT. When Kohn–Sham (KS) orbitals are used in second-order SAPT,[64,65] the total intermolecular interaction energy can be written as

$$E^{\mathrm{SAPT(KS)}}_{\mathrm{int}} = E^{(1)}_{\mathrm{elst}}(\mathrm{KS}) + E^{(1)}_{\mathrm{exch}}(\mathrm{KS}) + E^{(2)}_{\mathrm{ind,resp}}(\mathrm{KS}) + E^{(2)}_{\mathrm{exch-ind,resp}}(\mathrm{KS}) + E^{(2)}_{\mathrm{disp}}(\mathrm{KS}) + E^{(2)}_{\mathrm{exch-disp}}(\mathrm{KS}) + \delta \mathrm{E}^{\mathrm{HF}}_{\mathrm{int}} \tag{4}$$

The superscripts indicate the order in perturbation theory, and the "KS" indicates that intramolecular correlation is incorporated *via* DFT calculations for the monomers. The $\delta E^{\mathrm{HF}}_{\mathrm{int}}$ correction captures polarization effects beyond second order:

$$\delta E^{\mathrm{HF}}_{\mathrm{int}} = E^{\mathrm{HF}}_{\mathrm{int}} - [E^{(10)}_{\mathrm{elst}}(\mathrm{HF}) + E^{(10)}_{\mathrm{exch}}(\mathrm{HF}) + E^{(20)}_{\mathrm{ind,resp}}(\mathrm{HF}) + E^{(20)}_{\mathrm{exch-ind,resp}}(\mathrm{HF})] \tag{5}$$

Here, $E^{\mathrm{HF}}_{\mathrm{int}}$ is the counterpoise-corrected HF interaction energy, and the remaining energy components in eq 5 represent second-order SAPT applied to monomers described at the HF level. If desired, response ("resp") corrections can be included in the induction and exchange–induction terms in eqs 4 and 5, in order to capture orbital relaxation effects,[66,67] at some additional cost. In this study, the coupled induction and exchange–induction energies with orbital relaxation in SAPT-(KS) are approximated as[64]

DOI: 10.1021/acs.jctc.6b00155
J. Chem. Theory Comput. 2016, 12, 2569–2582

$$E^{(2)}_{\mathrm{ind,resp}}(\mathrm{KS}) = E^{(2)}_{\mathrm{ind}}(\mathrm{KS}) + E^{(20)}_{\mathrm{ind,resp}}(\mathrm{HF}) - E^{(20)}_{\mathrm{ind}}(\mathrm{HF}) \quad (6)$$

and

$$E^{(2)}_{\mathrm{exch-ind,resp}}(\mathrm{KS}) = E^{(2)}_{\mathrm{exch-ind}}(\mathrm{KS}) + E^{(20)}_{\mathrm{exch-ind,resp}}(\mathrm{HF}) - E^{(20)}_{\mathrm{exch-ind}}(\mathrm{HF}) \quad (7)$$

Second-order dispersion is the most expensive term in second-order SAPT(KS) and is also the least accurate.[68,69] (Cost to evaluate the other terms scales no worse than cubically with respect to system size.[53,70−72]) As in previous work,[19,69,73] we therefore replace the SAPT(KS) dispersion energy

$$E_{\mathrm{disp}} = E^{(2)}_{\mathrm{disp}}(\mathrm{KS}) + E^{(2)}_{\mathrm{exch-disp}}(\mathrm{KS}) \quad (8)$$

with our third-generation, SAPT-based dispersion potential ("+D3").[19] This is an empirical atom−atom dispersion potential that is fit to reproduce high-level SAPT2+3 dispersion energies for a training set of dimers, and is unrelated to Grimme's empirical +D3 correction for DFT.[74] Because the dispersion term is easily separable in SAPT, there is no double-counting problem in SAPT(KS)+D as there is in DFT+D, and the empirical dispersion potential in SAPT represents genuine dispersion, in contrast to the Grimme corrections.[62] This is an especially important point in the context of EDA, because it means that we can take the SAPT-based +D3 correction seriously as the dispersion contribution to the interaction energy.

It has been suggested[39,47] that a CT energy can be extracted from the SAPT induction energy by taking the difference between SAPT calculations in which the monomer wave functions are computed using the full dimer-centered basis set (DCBS), versus only the monomer-centered basis set (MCBS):

$$\Delta E^{\mathrm{SAPT}}_{\mathrm{CT}} = [E^{(2)}_{\mathrm{ind,resp}}(\mathrm{DCBS}) + E^{(2)}_{\mathrm{exch-ind,resp}}(\mathrm{DCBS})] - [E^{(2)}_{\mathrm{ind,resp}}(\mathrm{MCBS}) + E^{(2)}_{\mathrm{exch-ind,resp}}(\mathrm{MCBS})] \quad (9)$$

(The distinction between MCBS and DCBS is whether the SCF wave functions for the monomers are computed in a monomer basis or in a dimer basis containing ghost functions on the other monomer.) In principle, however, the correction defined in eq 9 vanishes in the limit of a complete basis set.[75]

Recently, Řezáč and de la Lande[52] have shown that when the CT energy is large; the higher-order induction terms included *via* the $\delta E^{\mathrm{HF}}_{\mathrm{int}}$ correction in eq 5 are actually dominated by CT. These authors suggest an alternative "SAPT+δSCF" procedure to define CT:

$$\Delta E^{\mathrm{SAPT}+\delta\mathrm{SCF}}_{\mathrm{CT}} = \Delta E^{\mathrm{SAPT}}_{\mathrm{CT}} + \delta E^{\mathrm{HF}}_{\mathrm{int}} \quad (10)$$

This should at least provide an upper bound for the CT interaction in second-order SAPT, since the two energy components in eq 10 are the only places where CT can appear.

IIC. Constrained DFT. Yet another way to define the CT interaction energy is to use the difference between the usual DFT energy of the dimer and the energy of a CT-free reference state that is constructed as a superposition of monomer densities, then relaxed subject to the constraint of no net charge flow between the monomers. The latter calculation is accomplished using cDFT.[50] This definition of the CT energy,

$$\Delta E^{\mathrm{cDFT}}_{\mathrm{CT}} = E^{\mathrm{DFT}} - E^{\mathrm{cDFT}} \quad (11)$$

was originally suggested by Wu et al.,[51] and revisited recently by Řezáč and de la Lande,[52] as a means to reduce or eliminate the basis-set dependence of the CT energy. This stability is achieved because there is no need to assign orbitals to one monomer or the other, and the basis set serves only to represent the density.

In early work on cDFT,[50,76−78] Mulliken or Löwdin atomic population analysis was typically used to assign electrons to atoms and thus to construct cDFT charge constraints, but this seems ill-advised in the present context because it would reintroduce orbitals into the definition of CT. Indeed, Mulliken-based cDFT in a def2-QZVPPD basis set yields $\Delta E^{\mathrm{cDFT}}_{\mathrm{CT}} = 0$ for water dimer,[52] a value that is unreasonable on its face, and especially so in view of numerous other EDAs (including several versions of ALMO-EDA) that predict CT energies ranging from −2.7 to −7.5 kJ/mol for this system.[79] (Natural bond orbital analysis[80] is an outlier in the opposite direction, predicting a significantly larger CT energy of −38.6 kJ/mol,[79] a fact that has been attributed to the nonvariational nature of the CT-free reference state in that approach.[14])

Alternatively, one can use a real-space partition of the density into atomic contributions by means of a weight function $w_{\mathrm{A}}(\mathbf{r})$ that defines a constraint

$$\int \mathrm{d}\mathbf{r}\, w_{\mathrm{A}}(\mathbf{r})\, \rho(\mathbf{r}) = N_{\mathrm{A}} \quad (12)$$

fixing the number of electrons on monomer A to be N_{A}. Both Becke[81] and Hirshfeld[82] partitions have been used in the context of cDFT to construct the function $w_{\mathrm{A}}(\mathbf{r})$,[50,83−85] and in particular Řezáč and de la Lande[52] use a "molecular Hirshfeld" approach with a weight function

$$w_{\mathrm{A}}(\mathbf{r}) = \frac{\rho_{\mathrm{A}}(\mathbf{r})}{\rho_{\mathrm{A}}(\mathbf{r}) + \rho_{\mathrm{B}}(\mathbf{r})} \quad (13)$$

Here, ρ_{A} and ρ_{B} are the densities of the isolated monomers A and B, computed at the geometries that these monomers have in the A···B complex. The cDFT procedure, with the weight function in eq 13, affords a CT energy of −3.3 kJ/mol for water dimer in the def2-QZVPD basis set,[52] a value that is well-aligned with other estimates cited above. In this work, however, we instead use the smooth Voronoi-type partition of real space introduced by Becke,[81] which yields much the same CT energy for water dimer (see section IVA). Regardless of how the function $w_{\mathrm{A}}(\mathbf{r})$ is chosen, the density $\rho(\mathbf{r})$ in eq 12 is the density of the interacting dimer, computed self-consistently in the presence of the constraint to obtain E^{cDFT} in eq 11. As such, the CT-free reference state is variational.

Horn and Head-Gordon[57] have recently clarified the meaning of the cDFT-based definition of CT introduced by Wu et al.[51] In Wu's work, the energy is partitioned as it is in ALMO-EDA (eq 1), with a frozen-density term supplemented by polarization and CT energies. However, the reference state for the frozen-density energy is different as compared to ALMO-EDA and, in ref 51, consists of a sum of monomer densities that is relaxed *subject to the constraint of fixed dimer density*. (This is possible within a Kohn−Sham framework and affects primarily the kinetic energy.) This relaxation process, which leads to a larger frozen-density energy in Wu et al.'s approach than in ALMO-EDA, introduces some "constant-density CT" into the frozen-density energy.[57] Subsequent use of cDFT to separate polarization from CT must, according to

DOI: 10.1021/acs.jctc.6b00155
J. Chem. Theory Comput. 2016, 12, 2569−2582

this argument, underestimate the energy-lowering that comes from CT, because it excludes the constant-density CT.

While this argument bears on the appropriate reference state for, and therefore definition of, the frozen-density energy, it has no bearing on SAPT/cDFT-EDA. In both ALMO-EDA and in the method of Wu et al.,[51] the frozen-density term contains the electrostatic, Pauli repulsion, and dispersion energies, yet each of these has a clear, separable, orbital-based definition in SAPT. In this work, cDFT is used in SAPT calculations only to separate induction from CT. Both ALMO-EDA and Wu's cDFT-based approach are fundamentally different partitions of the energy as compared to the SAPT/cDFT-EDA that is advocated here. The primary topic of this work is to examine the basis-set dependence of the ALMO- and SAPT/cDFT-EDAs.

III. COMPUTATIONAL DETAILS

BSSE must be removed in variational approaches such as ALMO-EDA,[29] *via* counterpoise correction.[42] The value of ΔE_{CT}^{cDFT} is only weakly dependent on basis set, as shown here and in ref 52, which indicates that the BSSE approximately cancels in eq 11, so no counterpoise correction is used in the cDFT calculations.

In ALMO-EDA, the frozen-density energy contains electrostatics, Pauli repulsion, and dispersion. As a result, this term can be rather sensitive to the choice of density functional, due primarily to inconsistent treatment of dispersion from one functional to the next. In systems such as $M^+\cdots C_6H_6$ and $M^+\cdots H_2O$, for example, we find that empirical Grimme-type +D corrections differ quite substantially from the pure dispersion potentials that we use in SAPT(KS)+D. In $K^+\cdots C_6H_6$, for example, the +D3 part of BLYP-D3 is only half as large as the SAPT-based dispersion correction (at the equilibrium separation), and the +D3 part of ωB97X-D3 is 13 times smaller than the SAPT correction.[37] We reiterate that only the +D correction in SAPT(KS)+D, which was fit directly to *ab initio* dispersion energies,[19] can safely be regarded as the actual dispersion component of the interaction energy. Grimme-style corrections are "model-dependent quantit[ies] with no real physical meaning".[62]

Recognizing the double-counting problem inherent in DFT +D, Szalewicz and co-workers[63] developed a "dispersionless" density functional (dlDF) by reparametrizing M05-2X using a data set of intermolecular interaction energies from which dispersion interactions were specifically removed *via* SAPT(DFT) calculations. (This should be contrasted with the ALMO-EDA approach to separating the dispersion interaction, eq 3, where HF theory is used as the "dispersionless" term.[30]) In our view, dlDF offers a relatively clean way to separate the dispersion energy in a DFT or DFT+D calculation, and dlDF can then be combined with our SAPT-based +D3 dispersion potential[19] to obtain a "dlDF+D3" method having no double-counting problem. Some results using this approach are presented herein.

ALMO and cDFT calculations reported here use either the B3LYP functional[86,87] or the ωB97X-D3 functional,[88] and cDFT calculations use noninteracting densities based on the Becke constraint to count electrons, as in refs 83 and 84. SCF-MI calculations (needed for ALMO-EDA) are based on the locally projected equations of Stoll et al.,[89] as implemented by Khaliullin et al.[60] For SAPT(KS), we use the LRC-ωPBE functional,[90,91] which has no short-range HF exchange, in conjunction with "ω_{GDD}" tuning of the range-separation parameter.[53,92] The SCF convergence criterion is set to 10^{-7} a.u. and the integral screening threshold is set to 10^{-12} a.u., using a fairly dense Euler−Maclaurin−Lebedev quadrature grid (N_{radial} = 75; $N_{angular}$ = 302). In the SAPT calculations, the *h* functions have been removed from aug-cc-pV5Z, and both the *h* and *i* functions are removed from aug-cc-pV6Z. In the ALMO and cDFT calculations, the *i* functions in aug-cc-pV6Z are removed. All calculations were performed using a locally modified version of Q-Chem,[93] in which we have recently implemented an open-shell version of SAPT.[53]

IV. RESULTS AND DISCUSSION

IVA. $(H_2O)_2$. The water dimer, which exhibits very little CT,[14,79] is a prototypical system for application of EDA to understand hydrogen bonding. Using a series of aug-cc-pVXZ basis sets, X = 2−6, we find that the electrostatic, exchange, and induction energies in SAPT are basically converged at the triple-ζ level, changing by <0.05 kJ/mol for X > 3. The ALMO-EDA polarization energy, in contrast, changes by 1.8 kJ/mol between X = 3 and X = 6.

Both experiments[10−12] and calculations[13,14] suggest that the CT interaction energy is approximately proportional to the amount of charge that is transferred, when averaged over the relative orientations of the interacting partners. The proportionality constant, *k* (energy per unit of transferred charge), can be estimated from state-of-the-art molecular-beam scattering experiments, albeit with some additional theoretical assumptions, primarily coming from theoretical charge-displacement analysis.[9] With this caveat, the experimental value inferred for *k* in the case of $Xe\cdots H_2O$ is $k = -2.6$ meV/me^-.[11] The authors of ref 11 suggest that the same value of *k* is also appropriate for the water dimer, in which case a CT energy for the water dimer of −3.6 kJ/mol is obtained based on the 14.6 me^- of charge that is transferred, according to charge-displacement analysis.[79] ALMO-EDA based on a coupled-cluster wave function [ALMO(CCSD)/aug-cc-pVTZ] affords a CT energy of −3.5 kJ/mol,[58] but larger basis sets have not been explored for ALMO(CCSD). Nevertheless, the ALMO(CCSD)/aug-cc-pVTZ value for the CT interaction in $(H_2O)_2$ is of the same order of magnitude as theoretical estimates from a variety of different EDAs.[79] As mentioned above, natural bond orbital analysis[80] represents an outlier for $(H_2O)_2$, predicting a CT energy of −38.6 kJ/mol, possibly due to the nonvariational nature of its CT-free reference state.[14] For this reason, natural bond orbital analysis will not be considered further in this work.

Unsurprisingly, CT energies for the orbital-based EDAs (SAPT and ALMO) are much more dependent on basis set as compared to the other energy components, as shown in Figure 2. Whereas the cDFT value of the CT energy is converged in a triple-ζ basis set, the SAPT- and ALMO-based values change by 1−3 kJ/mol between triple- and hextuple-ζ. Moreover, the cDFT value of ≈−3 kJ/mol is much closer to the experimental estimate as compared to ALMO(DFT) and SAPT. Řezáč and de la Lande[52] report a similar cDFT value (−3.3 kJ/mol) using a different functional, basis set, and charge-partition scheme.

A remark about basis-set recommendations is appropriate here. In both the original ALMO-EDA work[29] and later ALMO-EDA studies by Head-Gordon and co-workers,[14,30,57,94] including two studies on water dimer,[14,94] the aug-cc-pVQZ basis set is used extensively. More recently, however, Horn and Head-Gordon[56] suggest that "lack of a useful basis-set limit [for the separation of polarization from CT is] tempered by the use of basis sets with function spaces that were largely fragment-

DOI: 10.1021/acs.jctc.6b00155
J. Chem. Theory Comput. 2016, 12, 2569−2582

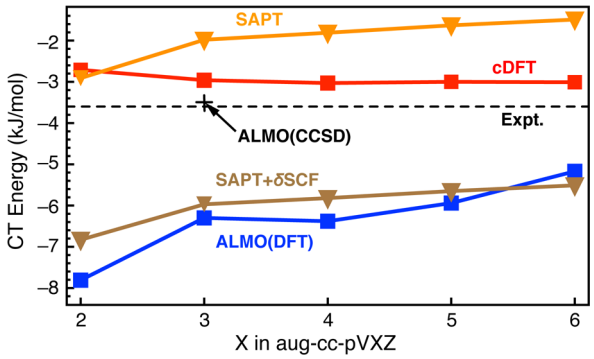

Figure 2. CT energies for $(H_2O)_2$ using a sequence of aug-cc-pVXZ basis sets, at the RI-MP2/aug-cc-pVDZ geometry of the dimer. The ωB97X-D3 functional is used for the ALMO(DFT) and cDFT calculations, and the LRC-ωPBE functional (with ω_{GDD} tuning[92]) is used for the SAPT and SAPT+δE_{int}^{HF} calculations. (Here "δSCF" denotes the δE_{int}^{HF} correction in eq 5.)

ascribable (*e.g.*, typically no larger than aug-cc-pVTZ)". In the present work, we are intentionally pushing both ALMO-EDA and SAPT beyond triple-ζ, in order to explore the basis-set limit (or lack thereof) for the CT term. From our point of view, a well-defined basis-set limit, and one that does not take the CT energy to zero, is an important feature of an EDA. The recent introduction of FERFs (see section IIA) as a new fragment-blocked basis for ALMO-EDA appears to mitigate the basis-set dependence in the case of water dimer,[56] but results have not been reported for the more challenging $H_3N\cdots BH_3$ system that is considered in section IVB, for which the CT energy is substantially larger than it is for $(H_2O)_2$.

As discussed above, ΔE_{CT}^{SAPT} should vanish, in principle, in the complete-basis limit, but for $(H_2O)_2$ it remains >1 kJ/mol in magnitude even in the aug-cc-pV6Z basis set, which illustrates just how slowly atom-centered basis sets converge to the basis-set limit. In contrast, $\Delta E_{CT}^{SAPT+\delta SCF}$ (eq 10) need *not* vanish in this limit, as the δE_{int}^{HF} correction need not vanish and typically converges in triple-ζ basis sets.

Figure 3a compares the CT interaction energies computed using cDFT versus ALMO-EDA. Use of B3LYP versus ωB97X-D3 makes only a minor difference of ≈1 kJ/mol in the ALMO-EDA case, and essentially no difference in the cDFT case. Figure 3b examines the amount of charge that is actually transferred in the ALMO calculations, using ALMO CT analysis.[13] Although the two functionals in question differ by about 0.5 me^- in their predictions, with B3LYP predicting slightly more CT, the dependence on basis set is virtually identical and also quite dramatic, decreasing monotonically as the basis set is enlarged. Only 2.3 me^- is transferred at the B3LYP/aug-cc-pV5Z level (consistent with results in ref 14), which seems unrealistic in comparison to the 14.6 me^- estimated from charge-displacement analysis.[79] As compared to the experimental results discussed above, it is interesting to note that ALMO-EDA underestimates the fraction of an electron that is transferred, yet overestimates the CT interaction energy, indicating that the proportionality constant k must be significantly overestimated as compared to the value estimated from experiment.

IVB. $H_3N\cdots BH_3$. The ammonia−borane complex is prototypical of dative bonding in a Lewis acid/base complex. It is a strongly interacting system, with SAPT electrostatic, exchange, and induction energies ranging from −200 to −500 kJ/mol, at least nine times larger than the corresponding energy

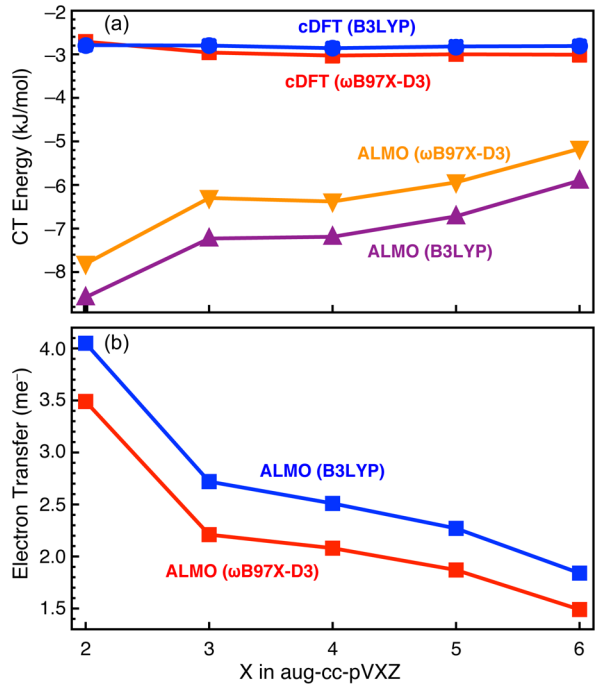

Figure 3. (a) CT energies for water dimer in a sequence of aug-cc-pVXZ basis sets. (b) Amount of charge that is transferred, as predicted by ALMO(DFT).

components in water dimer. As in $(H_2O)_2$, these energy components are essentially converged in a triple-ζ basis set, changing by at most 0.8 kJ/mol beyond aug-cc-pVTZ. For ALMO-EDA, the frozen-density and polarization energies range from −100 to −300 kJ/mol and are at least 25 times larger than the corresponding components in water dimer. However, the ALMO-EDA polarization energy is *not* converged at the triple-ζ level and changes by 36.3 kJ/mol upon enlarging the basis set from aug-cc-pVTZ to aug-cc-pV6Z. (The frozen-density energy changes only by 0.9 kJ/mol across the same range of basis sets.) This is consistent with the idea that the polarization energy is increasingly contaminated by charge transfer in the SCF-MI procedure, as the size of the basis set increases.[48]

CT energies for $H_3N\cdots BH_3$ are shown in Figure 4 as a function of basis set. For reference, the ALMO(CCSD)/aug-cc-

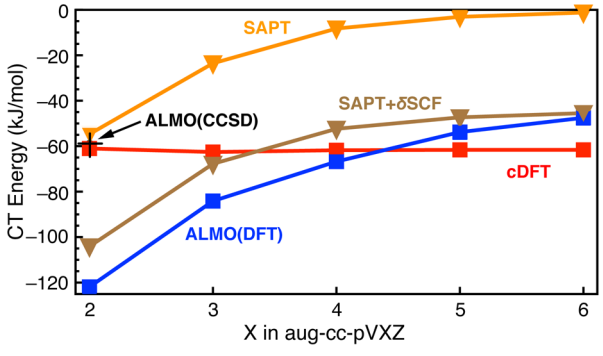

Figure 4. CT energies for $H_3N\cdots BH_3$ (RI-MP2/aug-cc-pVDZ geometry), in a sequence of aug-cc-pVXZ basis sets. The ωB97X-D3 functional is used for the ALMO(DFT) and cDFT calculations, and the LRC-ωPBE functional is used for the SAPT and SAPT+δSCF. The solid black cross represents the ALMO(CCSD)/aug-cc-pVDZ result.[58]

DOI: 10.1021/acs.jctc.6b00155
J. Chem. Theory Comput. 2016, 12, 2569−2582

pVDZ level of theory affords an estimate of −59.4 kJ/mol for the CT interaction.[58] The cDFT result is close to this value, at about −61 kJ/mol for all basis sets. CT energies from SAPT and ALMO(DFT) exhibit significant basis-set dependence, however, with the SAPT result ranging from −54.7 kJ/mol (aug-cc-pVDZ) to −1.2 kJ/mol (aug-cc-pV6Z), again converging toward zero in the basis-set limit. The δE_{int}^{HF} term converges to about −44 kJ/mol in aug-cc-pVTZ, so that this value will be the basis-set limit for the CT interaction as described by the SAPT+δE_{int}^{HF} method. The CT energy predicted by ALMO(DFT) ranges from −121.9 kJ/mol (aug-cc-pVDZ) to −47.5 kJ/mol (aug-cc-pV6Z), decreasing monotonically with basis size though not in a manner that suggests it will converge to zero.

Figure 5a compares cDFT and ALMO CT energies in the same sequence of basis sets, and Figure 5b plots the fraction of an electron that is actually transferred from ammonia to borane. Comparing ωB97X-D3 to B3LYP, we find that these quantities have only a weak dependence on the functional, but in the ALMO case both quantities are strongly dependent on the basis set. The fraction of an electron that is transferred ranges from 43.2 me^- (ωB97X-D3/aug-cc-pVDZ) to 9.5 me^- (aug-cc-pV6Z), with a large decrease in the CT interaction energy across the same range of basis sets. In contrast, cDFT results are basically independent of the basis set that is used.

IVC. Xe···H_2O. Experimental data on CT interaction energies for H_2O, NH_3, and H_2S in complexes with small molecules (N_2, O_2, and H_2) and rare-gas atoms are available from high-resolution, gas-phase scattering experiments, from which angle-averaged intermolecular potentials can be extracted.[10−12] Among these complexes, the CT interaction energy is largest in Xe···H_2O, at −0.98 kJ/mol,[11] which amounts to about 40% of the total interaction energy. The experiments afford a best-fit conversion factor k= −2.6 meV/me^-, and theoretical charge-displacement analysis suggests 3.9 me^- of charge is transferred from Xe to H_2O. Figure 6 shows CT energies in Xe···H_2O computed using ALMO-, cDFT-, and SAPT-based methods in two different basis sets. The ALMO(DFT) method dramatically overestimates the experimental CT energy in a triple-ζ basis set and affords a much different result in quadruple-ζ basis set.

According to ALMO-based CT analysis, the ALMO(DFT) calculation transfers 1.8 me^- (triple-ζ) or 0.8 me^- (quadruple-ζ), as compared to 3.9 me^- in charge-displacement analysis,[11] nevertheless the ALMO CT interaction energy is larger than the experimental one. As with water dimer, this suggests that ALMO(DFT) significantly overestimates the value of k. (It has previously been suggested that ALMO may underestimate the CT energy due to mixing in with polarization,[49] but the minuteness of the polarization energy for Xe···H_2O means this cannot be the case here.)

IVD. M^+···H_2O and M^+···C_6H_6. Although it is difficult to obtain reliable reference data to assess the accuracy of various models for the CT interaction energy, an EDA should at least produce results that agree with chemical intuition in obvious cases, exemplified here by M^+···H_2O and M^+···C_6H_6 complexes with M = Li, Na, or K. We call these "obvious" cases because we expect that the smaller alkali metal cations should approach more closely to the molecule and thus more effectively withdraw charge, and as such we expect the CT energy to decrease as one moves down the group I cations, due to increasing ion−molecule distance. Results in Figure 7 reveal that only cDFT reproduces this anticipated trend.

In contrast, ALMO calculations show no trend at all. Different results (in different basis sets) for M^+···H_2O have been reported in ALMO calculations by Phipps et al.,[37] who found that the CT energy was largest for M = K, even in the smallest basis set employed in that study. In the quadruple-ζ basis set used here, the ALMO CT energy is largest for M = Li. Phipps et al. argue that the unphysical behavior they observe in M^+···H_2O might be an artifact of counterpoise correction, but in our calculations the counterpoise corrections for M = Li, Na, and K in M^+···H_2O, amount to only 0.06, 0.09, and 0.14 kJ/mol, respectively, all of which are small in comparison to the ALMO CT energies reported in Figure 7a.

The SAPT CT energies for these systems are also rather strange, as they are repulsive in several cases. For both H_2O and C_6H_6, the δE_{int}^{HF} correction is negative for Li^+ and K^+ but

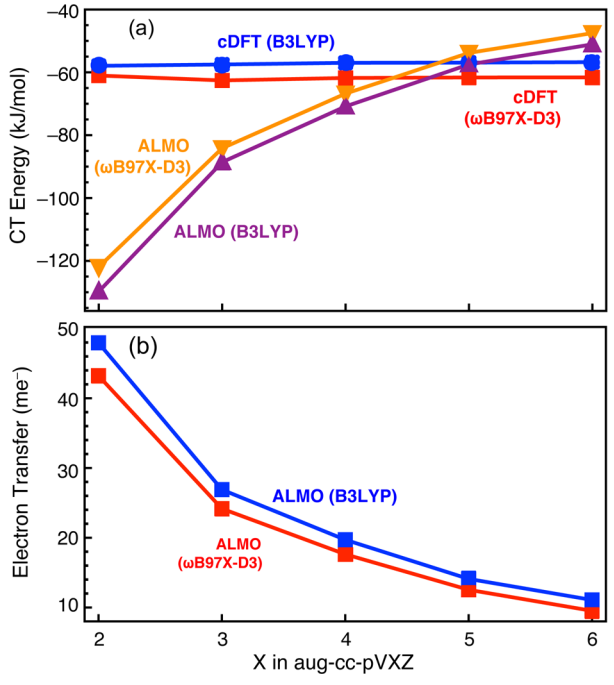

Figure 5. (a) CT energies for H_3N···BH_3 using ALMO(DFT) and cDFT in a variety of basis sets. (b) Amount of charge that is transferred, as predicted by ALMO CT analysis.[13]

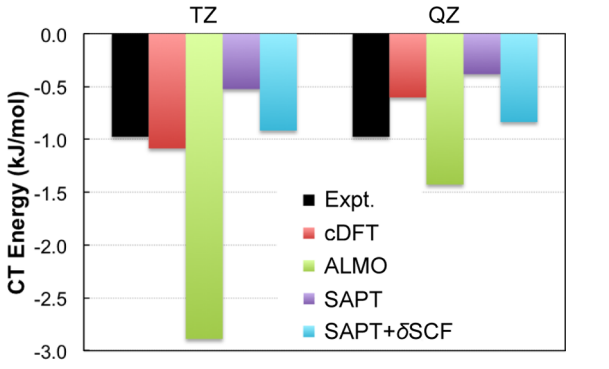

Figure 6. CT energies for Xe···H_2O, using the ωB97X-D3 functional for the ALMO(DFT) and cDFT calculations and the LRC-ωPBE functional for the SAPT and SAPT+δSCF. The "TZ" basis set is aug-cc-pVTZ for H_2O and def2-TZVPPD for Xe, and "QZ" is aug-cc-pVQZ for H_2O and def2-QZVPPD for Xe. The geometry of the complex is taken from ref 11.

DOI: 10.1021/acs.jctc.6b00155
J. Chem. Theory Comput. 2016, 12, 2569−2582

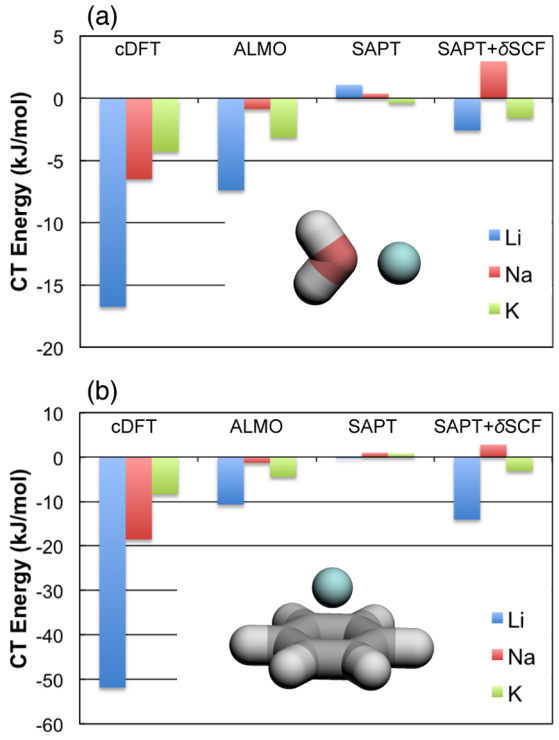

Figure 7. CT energies for (a) $M^+\cdots H_2O$ and (b) $M^+\cdots C_6H_6$. The ωB97X-D3 functional is used for the ALMO(DFT) and cDFT calculations, and the LRC-ωPBE functional is used for SAPT and SAPT+δSCF. In panel a, the aug-cc-pVQZ basis set is used for H_2O and the def2-QZVPPD basis set is used for M^+, whereas in panel b aug-cc-pVTZ is used for benzene and def2-TZVPPD for M^+. Geometries were optimized at the RI-MP2 level using the analogous double-ζ basis sets.

positive for Na^+, with the result that the SAPT+δE_{int}^{HF} CT energies (like the ALMO ones) exhibit no trend across group I. In short, none of the orbital-based definitions of the CT energy follows the expected trend across group I, but this trend *is* reproduced by cDFT.

IVE. Charge-Transfer Complexes. Řezáč and de la Lande[52] have assembled a set of 11 dimers that span a wide range of CT energies and used them to test the performance of cDFT using generalized gradient approximation (GGA) and meta-GGA functionals, but not hybrids. We will use the same data set to test the methods examined here. Following ref 52, we estimate the fractional charge transfer δq using atomic charges from natural population analysis[95] (NPA) at the HF/cc-pVTZ level, with charges obtained from ref 96. Figure 8 plots the CT energies for this data set. All of the methods examined here are in rough agreement (and exhibit similar trends) when $\delta q < 0.1\ e^-$, but in the four cases where δq is largest, the CT energies (and even the trends) vary widely. Of the methods in Figure 8, cDFT affords the best linear correlation between δq and the CT interaction energy, with a correlation coefficient $R^2 = 0.98$.

IVF. Cation–Alkyl Radical Complexes. Next we examine CT energies for open-shell systems in order to make contact with the rich chemistry of radicals. Complexes involving alkyl radicals such as $CH_3^\bullet$ and $(CH_3)_3C^\bullet$, stabilized by cations (H_3O^+ or NH_4^+ in this work) are interesting model systems for understanding the stabilization of transition structures in reactions involving proteins.[3,97] These complexes are also interesting from the standpoint of CT analysis, since electron-

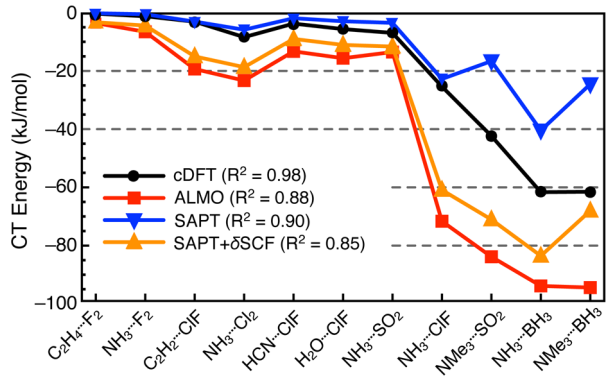

Figure 8. CT energies computed using the def2-QZVPPD basis set. The ωB97X-D3 functional is used for the cDFT and ALMO calculations, and LRC-ωPBE is used for the SAPT and SAPT+δSCF calculations. Also listed are the R^2 goodness-of-fit parameters for a linear fit of the CT energy versus the fractional charge δq that is transferred, as determined using NPA atomic charges. The four dimers on the far right are the only ones for which $\delta q > 0.1\ e^-$.

deficient radicals often have energetically low-lying singly occupied MOs than can accept some fraction of an electron from a donor molecule. To compare open- versus closed-shell interactions, we will also examine the corresponding closed-shell species, CH_4 and $(CH_3)_3CH$. The eight complexes considered here are shown in Figure 9 and have previously been examined using ALMO-EDA in ref 49. That study used B3LYP, whereas we use ωB97X-D3, which systematically reduces the CT interaction energies by an average of 2.5 kJ/mol. This is consistent with the idea that delocalization error,[98,99] which manifests in EDA as an exaggeration of CT interactions,[100,101] is reduced in ωB97X-D3 as compared to B3LYP.

Chemically and qualitatively, one expects the CT interaction energy to be determined by the IE of the donor species and the EA of the acceptor, with a strong dependence on intermolecular distance and mutual orientation.[3] In Figure 10 we plot CT interaction energies versus the inverse donor–acceptor gap, $(IE - EA)^{-1}$. Very good linear correlations are obtained, with R^2 values close to unity for each method examined. (The R^2 values using SAPT alone are a bit smaller, although $R^2 \approx 1$ upon addition of the δE_{int}^{HF} correction.) Note in particular that cDFT affords the best fits of all, with $R^2 > 0.99$.

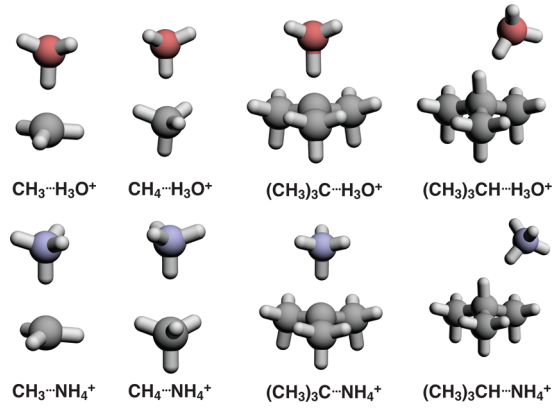

Figure 9. Complexes of $CH_3^\bullet$, $(CH_3)_3C^\bullet$, CH_4, and $(CH_3)_3CH$ with H_3O^+ or NH_4^+. Geometries are taken from ref 49.

DOI: 10.1021/acs.jctc.6b00155
J. Chem. Theory Comput. 2016, 12, 2569–2582

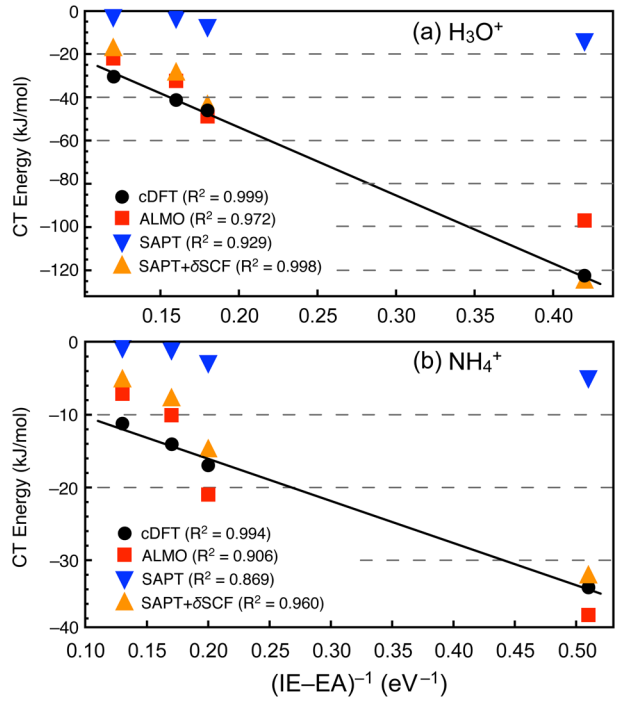

Figure 10. CT energies for the cation−molecule and cation−radical complexes in Figure 9, plotted as a function of the inverse donor−acceptor gap. The ωB97X-D3/def2-QZVPPD level of theory is used for ALMO and cDFT calculations, and LRC-ωPBE/def2-QZVPPD is used for SAPT and SAPT+δSCF. Also listed are R^2 values for linear fits of the data, with the linear fit shown for cDFT.

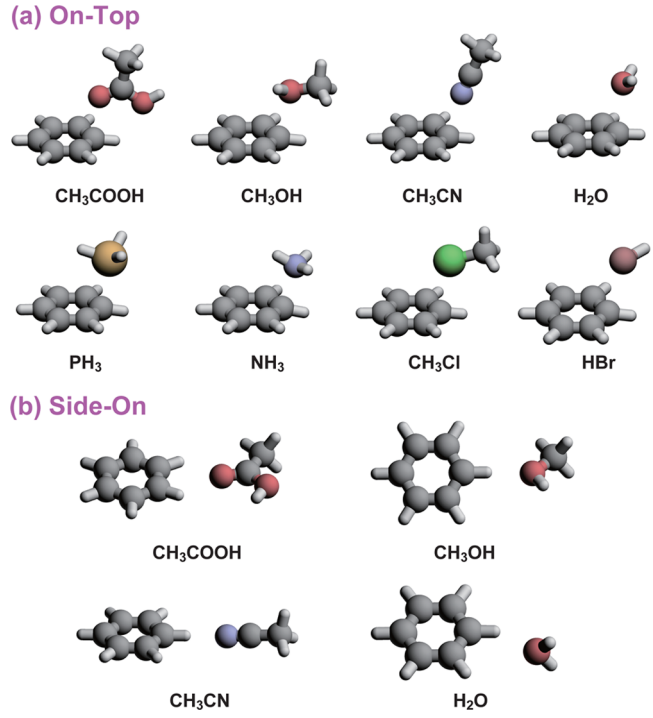

Figure 11. Complexes of $C_6H_6^{\bullet+}$ with various nucleophiles, in the "on-top" and "side-on" configurations. Geometries are taken from ref 49.

This suggests an easy way to estimate the magnitude of the CT energy, based on calculations performed on the isolated species.

IVG. Nucleophile−$C_6H_6^{\bullet+}$ Complexes. Interaction between oxidized aromatic rings (such as damaged DNA bases) and nucleophiles (such as water or alcohol) play key roles in many biochemical reactions.[102,103] The aryl radical, $C_6H_6^{\bullet+}$, has two different binding sites that behave differently during nucleophilic aromatic substitution reactions at the radical center.[104] ALMO-EDA has previously been used to examine these "on-top" versus "side-on" configurations in complexes spanning a wide range of IEs,[49] and we will examine the same complexes here. These complexes are depicted in Figure 11.

CT energies for $C_6H_6^{\bullet+}$ with eight different nucleophiles oriented in the on-top position are plotted versus $(IE - EA)^{-1}$ in Figure 12. Linear fits of the data afford $R^2 \approx 1$, but we note in particular that inclusion of the δE_{int}^{HF} term in the SAPT calculation improves the value of R^2 significantly, as was the case for the cation−alkyl radical complexes. While the *correlations* are significant for each of the EDAs in Figure 12, different approaches afford very different *values* for the CT energy, especially when the donor/acceptor gap is small. Excluding the SAPT results without δE_{int}^{HF} (since the CT energies in this approach are all relatively small), the remaining three methods span a range of 39 kJ/mol for $C_6H_6^{\bullet+}\cdots PH_3$, the system for which the gap is smallest.

CT energies for the side-on orientations of these complexes are considerably smaller, ranging from −4.0 to −5.6 kJ/mol in cDFT calculations, which is probably due to unfavorable overlap. Regardless of which EDA is used, these CT energies are less strongly correlated with the inverse gap as compared to the on-top configurations (see Table S2 in the Supporting Information), though this may be due to the limited number of data points in the side-on case.

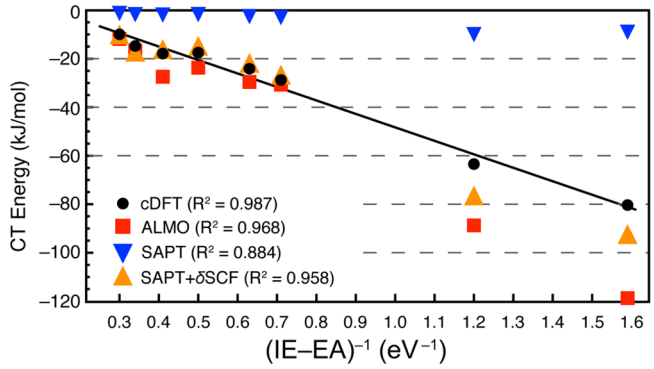

Figure 12. CT energies for $C_6H_6^{\bullet+}$ complexes with various nucleophiles in the on-top configuration, as a function of the inverse gap $(IE - EA)^{-1}$, where IE is the ionization energy of the nucleophile and EA denotes the electron affinity of $C_6H_6^{\bullet+}$, that is, the IE of benzene. (IE and EA data are taken from ref 105.) The ωB97X-D3/def2-QZVPPD method is used for the ALMO and cDFT calculations, and LRC-ωPBE/def2-QZVPPD is used for SAPT and SAPT+δSCF.

The binding energy of $C_6H_6^{\bullet+}\cdots H_2O$ is nearly the same in both the on-top and side-on orientations and has previously been analyzed using ALMO-EDA with the conclusion that the side-on interaction is dominated by the frozen-density term while the on-top interaction has a large CT component.[49] We repeated the B3LYP calculations from ref 49 for these two isomers, and in Table 1 we also report ALMO-EDA using ωB97X-D3 and the dlDF functional. All three functionals predict similar values for the total interaction energy, and all three predict a frozen-density energy that is larger in the side-on orientation but a CT energy that is larger in the on-top configuration. (The ωB97X-D3 functional does predict less CT as compared to B3LYP, consistent with a larger delocalization

DOI: 10.1021/acs.jctc.6b00155
J. Chem. Theory Comput. 2016, 12, 2569−2582

Table 1. ALMO Energy Components[a] for $C_6H_6^{\bullet+}\cdots H_2O$ in Two Orientations

		energy component (kJ/mol)				
orientation	functional	FRZ	POL	CT	DISP[b]	total
on-top	B3LYP	−11.1	−7.9	−17.0		−36.0
	ωB97X-D3	−21.6	−8.4	−12.1		−42.1
	dlDF	−4.9	−8.3	−8.0	−20.1	−41.3
side-on	B3LYP	−25.3	−6.9	−4.7		−36.9
	ωB97X-D3	−30.4	−7.2	−4.0		−41.5
	dlDF	−20.8	−6.8	−3.5	−11.1	−42.2

[a]6-311++G(3df,3pd) basis set. [b]The dispersion energy is normally unavailable for ALMO and for dlDF is evaluated at the SAPT2+3-(CCD)/aug-cc-pVTZ level for the closed-shell $C_6H_6\cdots H_2O$ complex.

error for the latter.) However, dlDF predicts a frozen-density energy that is far less attractive as compared to that obtained with either of the other two functionals, which is compensated for by the dispersion energy. For use with dlDF, we estimate the dispersion energy *via* a high-level SAPT2+3(CCD)/aug-cc-pVTZ calculation for the closed-shell $C_6H_6\cdots H_2O$ complex, since SAPT beyond second order has only been implemented for closed-shell systems. Calculations using the Becke−Johnson exchange-dipole model (XDM),[106,107] which *is* available for open-shell systems, suggest that substituting the closed-shell system changes the dispersion energy by <1 kJ/mol; see the Supporting Information. We do not analyze these discrepancies among functionals in any further detail, because further decomposition of the frozen-density energy has only just become possible,[30] after the present work was submitted for publication.

SAPT results for the two $C_6H_6^{\bullet+}\cdots H_2O$ complexes are listed in Table 2. As in the DFT calculations discussed above, interaction energies for the two orientations are similar in either orientation, but here we obtain a more detailed picture. According to SAPT, the electrostatic interactions are similar, but the on-top configuration is destabilized by Pauli repulsion (EXCH in Table 2) to a much greater extent. This is consistent with a shorter intermolecular distance in the on-top configuration: 3.2 Å versus 4.5 Å between monomer centers of mass. This explains why the frozen-density energies in Table 1 are less stabilizing in the on-top case, as the Pauli repulsion is contained in this term.

A final remark is that we expect the CT interaction to somehow correlate with donor/acceptor "overlap", however that might be defined. In the ALMO-EDA case, we might assess such a relationship by examining the correlation between the CT energy and the frozen-density energy, since the latter contains the Pauli repulsion. The analogous exercise with SAPT/cDFT-EDA is to examine the correlation between the cDFT CT energy and the SAPT exchange energy. These two comparisons are plotted in Figure 13 for both the on-top and side-on orientations of the $C_6H_6^{\bullet+}\cdots$nucleophile data set. In the SAPT case, CT is strongly correlated with the exchange energy (R^2 = 0.95) but the correlation is somewhat less significant (R^2 = 0.83) in the ALMO-EDA case, perhaps because the exchange energy is mixed up with electrostatics and dispersion in the frozen-density energy.

Table 2. Energy Components for $C_6H_6^{\bullet+}\cdots H_2O$ Based on Open-Shell SAPT[a]

	energy component (kJ/mol)					
	ELST	EXCH	IND		DISP[c]	total
orientation			total	CT[b]		
on-top	−48.5	43.2	−17.2	−10.1	−20.1	−42.6
side-on	−46.7	25.1	−10.9	−4.0	−11.1	−43.5

[a]Using LRC-ωPBE/def2-QZVPPD for the ELST, EXCH, and IND components. [b]Based on cDFT at the level of ωB97X-D3/def2-QZVPPD. [c]Evaluated at the SAPT2+3(CCD)/aug-cc-pVTZ level for $C_6H_6\cdots H_2O$.

IVH. $C_{10}H_8^{\bullet+}\cdots C_6H_6$. A final example is the complex between benzene and the naphthalene radical cation, for which ΔH° = 33 ± 4 kJ/mol has recently been measured experimentally.[108] This and related cation radical dimers of aromatic hydrocarbons are good model systems to understand the basis of photoconductivity and ferromagnetism in organic materials.[109−111] Enthalpies of binding for the homodimers $C_6H_6^{\bullet+}\cdots C_6H_6$ (ΔH° = 71 kJ/mol) and $C_{10}H_8^{\bullet+}\cdots C_{10}H_8$ (ΔH° = 74.5 kJ/mol) are much larger,[112] and the smaller binding energy for $C_{10}H_8^{\bullet+}\cdots C_6H_6$ has been explained in terms of a large degree of charge delocalization in naphthalene as compared to benzene, which reduces the CT interaction in the former.[108] The large difference in IE between naphthalene (8.1 eV) and benzene (9.2 eV) is taken as evidence of the lack of charge−resonance interaction in (naphthalene)$^{\bullet+}\cdots$benzene,[108] whereas this effect is obviously in play for the homodimers. Given such a large difference in IEs, however, one would not expect much CT either, but ALMO-EDA with the M11 functional[113] and cc-pVTZ basis set predicts a surprisingly large CT interaction for this complex in its face-to-face arrangement.[108] Three different isomers of $C_{10}H_8^{\bullet+}\cdots C_6H_6$ (as shown in Figure 14) are considered here, in order to

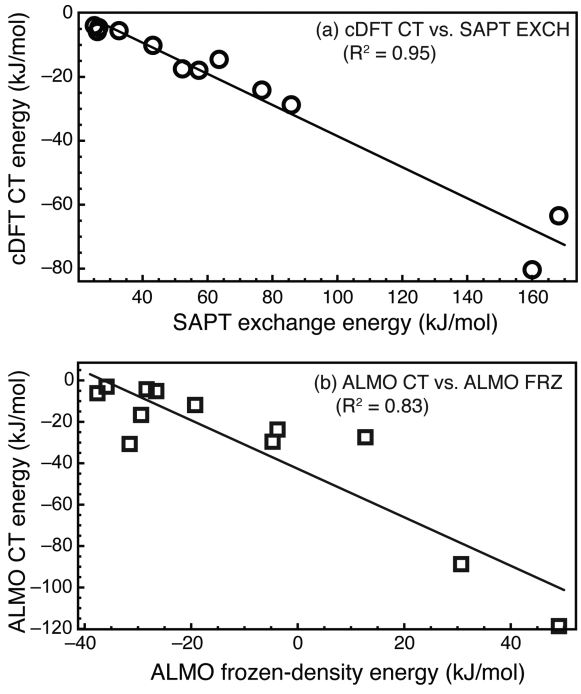

Figure 13. (a) CT energies from cDFT versus SAPT exchange energies and (b) CT energies from ALMO-EDA versus ALMO frozen-density energies, for all 12 $C_6H_6^{\bullet+}\cdots$nucleophile complexes in Figure 11. The ωB97X-D3/def2-QZVPPD level of theory is used for the ALMO and cDFT calculations, and LRC-ωPBE/def2-QZVPPD is used for SAPT calculations. Linear fits and corresponding R^2 values are indicated.

DOI: 10.1021/acs.jctc.6b00155
J. Chem. Theory Comput. 2016, 12, 2569−2582

assess whether this unusually large CT interaction is a general trend amongst EDAs or is specific to ALMO-EDA.

ALMO-EDA results for these three isomers, using both ωB97X-D3 and dlDF, are listed in Table 3. The polarization interaction is similar for all three isomers but the frozen-density term varies, and results for the two functionals are quite different. Using dlDF we can safely disentangle the dispersion energy from the frozen-density energy, and we accomplish this using an atom−atom dispersion potential that is fit to high-level SAPT calculations for a training set of small dimers, namely, the +D3 potential of ref 19, which is the same dispersion correction used elsewhere in this work for SAPT(KS)+D. Results suggest that the face-to-face F0 arrangement exhibits a dispersion interaction about twice as large as the other two configurations, which is consistent with results for benzene dimer,[114] where π-stacked configurations exhibit larger dispersion interactions as compared to T-shaped isomers. This is due to the rapid decay of dispersion with distance and the fact that stacked configurations put more of the π electron clouds of the two monomers into close proximity.

Despite our earlier admonitions against interpreting Grimme-style +D corrections as true dispersion, as an illustrative exercise we have done just that for the ωB97X-D3 results in Table 3. (The D3 correction is then subtracted from the frozen-density energy.) The frozen-density term in dlDF is repulsive for all three isomers, but about 2−3 times more repulsive for F0 than for the other two isomers. This is consistent with the shorter intermolecular separation for F0. In the case of ωB97X-D3, however, the frozen-density energy (*sans* D3) is far less repulsive than it is for dlDF, and even slightly attractive for the other two isomers. That the total interaction energies are roughly the same for both functionals is a consequence of an empirical +D3 correction in ωB97X-D3 that is much less attractive than the SAPT-based +D3 correction that we append to dlDF. This example provides a vivid demonstration of the disparity between empirical corrections and SAPT-based dispersion potentials. Given the documented accuracy of the latter,[19] it illustrates why the empirical corrections should not be conflated with true dispersion energies.

Turning now to the CT interaction energy, our ALMO-EDA calculations suggest it is about twice as large for isomer F0 as that for V0, and three times as large as that in S0. This is consistent with previous ALMO-EDA results that noted the "unexpectedly high CT" in the face-to-face arrangement.[108] Other estimates of CT interaction energies for these three dimers can be found in Table 4. SAPT values for the CT energy are negligible for all three isomers but are larger (and similar to ALMO-EDA results) when the δE_{int}^{HF} correction is included.

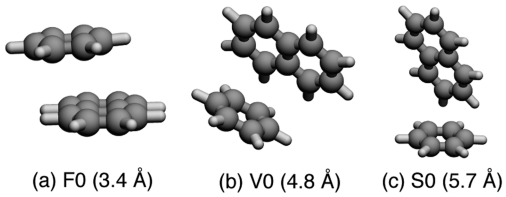

Figure 14. Lowest-energy structures for each of three classes of isomers of $C_{10}H_8^{\bullet+}\cdots C_6H_6$: (a) face-to-face, (b) V-shaped, and (c) face-to-side. Geometries are taken from ref 108, and the value in parentheses represents the distance between monomer centers of mass.

Table 3. ALMO-EDA Results[a] for Three Isomers of (Naphthalene)$^{\bullet+}$···(Benzene)

		energy component (kJ/mol)				
isomer	functional	FRZ[b]	POL	CT	DISP[c]	total
F0	ωB97X-D3	15.2	−14.0	−17.7	−24.6	−41.1
	dlDF-D3	57.3	−9.4	−16.0	−66.9	−35.0
V0	ωB97X-D3	−1.6	−15.0	−6.9	−14.4	−38.0
	dlDF-D3	22.2	−10.9	−7.1	−36.2	−32.0
S0	ωB97X-D3	−3.1	−12.4	−5.8	−11.1	−32.4
	dlDF-D3	16.5	−8.9	−5.4	−29.2	−27.1

[a]def2-TZVPPD basis set. [b]DISP energy has been subtracted from FRZ for ωB97X-D3. [c]Computed using the Grimme-style +D3 correction for ωB97X-D3, and using the SAPT-based +D3 potential of ref 19 for dlDF-D3.

Table 4. CT Interaction Energies (kJ/mol) for (Naphthalene)$^{\bullet+}$···(Benzene)

method	F0	V0	S0
cDFT[a]	−9.0	−6.4	−5.0
ALMO[a]	−17.7	−6.9	−5.8
SAPT[b]	−0.5	−0.4	−0.3
SAPT[b]+δE_{int}^{HF}	−17.4	−8.8	−6.4

[a]ωB97X-D3/def2-TZVPPD level. [b]LRC-ωPBE/def2-TZVPPD level with ω_{GDD} tuning.

However, the more robust cDFT approach affords CT energies that are considerably smaller and amount to 22% of the total interaction energy for F0 and 15% for S0. This should be compared to ALMO(ωB97X-D3) results where 43% of the F0 interaction energy is assigned to CT and 18% for S0. The cDFT calculations do not support the idea of unusually large CT in the face-to-face arrangement.

In Table 5, we put forward a hybrid energy decomposition scheme (as applied to $C_{10}H_8^{\bullet+}\cdots C_6H_6$) in which a SAPT(KS)+D3 calculation is used to obtain the electrostatic, Pauli repulsion, induction, and dispersion components, with the latter corresponding precisely to the SAPT-based +D3 correction.[19] At this level, the CT energy is contained within the induction term, so we then reduce the SAPT induction energy by the CT interaction obtained using cDFT. We propose that the SAPT(KS) induction energy, less the cDFT estimate of the CT energy, be taken as the actual (CT-free) induction energy.

A previous ALMO-EDA study of $C_{10}H_8^{\bullet+}\cdots C_6H_6$ found that isomer F0 has the smallest (least attractive) frozen-density interaction,[108] consistent with our ALMO-EDA results in Table

Table 5. Energy Components for Three Isomers of $C_{10}H_8^{\bullet+}\cdots C_6H_6$ Based on Open-Shell SAPT(KS)+D3/cDFT Calculations

	energy component (kJ/mol)					
	ELST[a]	EXCH[a]	IND		DISP[c]	total
isomer			total[a]	CT[b]		
F0	−39.3	79.4	−25.2	−9.0	−66.9	−52.0
V0	−29.2	41.7	−19.1	−6.4	−36.2	−42.8
S0	−25.3	33.4	−15.1	−5.0	−29.2	−36.1

[a]From SAPT(KS) using LRC-ωPBE/def2-TZVPPD. [b]Using cDFT at the ωB97X-D3/def2-TZVPPD level. [c]Using the SAPT-based +D3 potential of ref 19.

DOI: 10.1021/acs.jctc.6b00155
J. Chem. Theory Comput. 2016, 12, 2569−2582

3. This fact was attributed to electrostatics,[108] with the authors speculating that perhaps the charge−quadrupole interaction is smallest in the F0 isomer. However, with SAPT we can extract the actual electrostatic component, which in ALMO is buried in the frozen-density term. We find that the SAPT electrostatic energy is actually *most* stabilizing for F0 (see Table 5). This is consistent with SAPT2+/aug-cc-pVTZ results for protonated benzene dimer,[115] which exhibits similar geometric binding motifs. In that system, the electrostatic interaction is strongest in the parallel-displaced arrangement that is qualitatively similar to the F0 isomer of $C_{10}H_8^{\bullet+}\cdots C_6H_6$.

The energy decomposition in Table 5 paints an interesting picture of the balance of forces that determines the relative energies of F0, V0, and S0. The F0 isomer exhibits the largest dispersion interaction, as a result of the relatively close proximity of the π-electron clouds as compared to the V0 and S0 isomers. This is probably also the reason why the induction interaction is most favorable in F0, due to polarization of benzene's π electrons from the positive charge on the naphthalene cation. At the same time, F0 exhibits the shortest intermolecular separation (measured as the distance between monomer centers of mass), and hence the largest value of the Pauli repulsion. This partially offsets the more favorable electrostatic, induction, and dispersion interactions, to the point where total interaction energies amongst the three isomers are not so disparate. We also note that the CT contributions to the binding energies, when computed using our SAPT/cDFT scheme, are rather small, consistent with chemical intuition given the large difference in the IEs of the two neutral monomers.

V. CONCLUSIONS

We have examined several orbital-based EDAs that are designed to decompose intermolecular interaction energies into physically meaningful components. These have been compared to constrained DFT calculations, specifically in the context of how these methods quantify CT interactions. Ultimately, we recommend the cDFT-based definition of the CT interaction energy in conjunction with a SAPT-based definition of the remaining energy components, with the SAPT induction (polarization) energy reduced in magnitude by the cDFT CT energy. This combined SAPT/cDFT-EDA has several distinct advantages:

(1) It exhibits very little basis-set dependence, in contrast to orbital-based (ALMO or plain SAPT) definitions, and the CT interaction does not vanish in the basis-set limit as it does in traditional SAPT. Some progress has been made quite recently to reduce the basis-set dependence of ALMO-EDA calculations,[56] and it will be interesting to see how future versions of ALMO-EDA compare to SAPT/cDFT-EDA.

(2) It provides quantitative CT results for $(H_2O)_2$, $H_3N\cdots BH_3$, and $Xe\cdots H_2O$, as compared to the best values in the literature, including experimental estimates of the CT interaction energy.

(3) For $M^+\cdots H_2O$ and $M^+\cdots C_6H_6$ complexes, it provides a chemically intuitive trend across the group I alkali cations M^+, with CT interaction energies decreasing with increased distance. ALMO-EDA and plain SAPT exhibit no clear trend across group I.

(4) In open-shell complexes, predicted CT energies exhibit excellent correlation with the inverse donor/acceptor gap, $(IE - EA)^{-1}$.

(5) It can rationalize the relative binding energies for isomers of the radical cation complex (benzene)···(naphthalene)$^{\bullet+}$, and resolves an anomaly wherein ALMO-EDA predicts curiously large CT interaction energies that do not correlate with the ionization energies of the neutral monomers.

(6) CT interaction energies computed with the cDFT procedure endorsed here, which uses hybrid functionals, correlate better with the amount of charge that is transferred, as compared to previous cDFT calculations using GGA functionals.[52]

In summary, we recommend a composite SAPT(KS)+D3/cDFT scheme as a robust procedure for analyzing intermolecular interactions. In this approach, the dispersion energy is provided by an accurate and *nonempirical* atom−atom dispersion potential,[19] fit to third-order SAPT calculations. Should the accuracy of the +D3 dispersion potential ever be in doubt, however, SAPT/cDFT-EDA is seamlessly compatible (albeit at increased cost) with the use of either third-order SAPT,[39] SAPT(DFT),[40,41] or other approaches to computing the dispersion component of the interaction energy.

■ ASSOCIATED CONTENT

Supporting Information

The Supporting Information is available free of charge on the ACS Publications website at DOI: 10.1021/acs.jctc.6b00155.

Additional tests of basis-set dependence, XDM calculations, and CT interaction energies for the cation−alkyl radical and nucleophile−aryl radical complexes (PDF)

■ AUTHOR INFORMATION

Corresponding Author

*E-mail: herbert@chemistry.ohio-state.edu.

Funding

This work was supported by the U.S. Department of Energy, Office of Basic Energy Sciences, Division of Chemical Sciences, Geosciences, and Biosciences under Award No. DE-SC0008550. Calculations were performed at the Ohio Supercomputer Center under Project PAA-0003.[116] K.U.L. acknowledges support from a Presidential Fellowship awarded by The Ohio State University.

Notes

The authors declare the following competing financial interest(s): J.M.H. serves on the Board of Directors of Q-Chem, Inc.

■ ACKNOWLEDGMENTS

J.M.H. is a Camille Dreyfus Teacher-Scholar and a fellow of the Alexander von Humboldt Foundation. We thank Dr. Jan Řezáč for providing geometries for the CT complexes in Section IVE, from ref 52.

■ REFERENCES

(1) de Visser, S. P.; Shaik, S. *J. Am. Chem. Soc.* **2003**, *125*, 7413−7424.

(2) Wang, B.-Q.; Li, Z.-R.; Wu, D.; Hao, X.-Y.; Li, R.-J.; Sun, C.-C. *Chem. Phys. Lett.* **2003**, *375*, 91−95.

(3) Hammerum, S. *J. Am. Chem. Soc.* **2009**, *131*, 8627−8635.

(4) Li, Q.-Z.; Li, H.-B. In *Noncovalent Forces*; Scheiner, S., Ed.; Challenges and Advances in Computational Chemistry and Physics, Vol. *19*; Springer: Heidelberg, Germany, 2015; pp 107−127, DOI: 10.1007/978-3-319-14163-3_5.

DOI: 10.1021/acs.jctc.6b00155
J. Chem. Theory Comput. 2016, 12, 2569−2582

(5) Boozer, C. E.; Hammond, G. S. *J. Am. Chem. Soc.* **1954**, *76*, 3861−3862.
(6) Russell, G. A. *J. Am. Chem. Soc.* **1958**, *80*, 4987−4996.
(7) Knowles, R. R.; Jacobsen, E. N. *Proc. Natl. Acad. Sci. U. S. A.* **2010**, *107*, 20678−20685.
(8) Lu, T.; Wheeler, S. E. *Science* **2015**, *347*, 719−720.
(9) Bistoni, G.; Belpassi, L.; Tarantelli, F. *J. Chem. Theory Comput.* **2016**, *12*, 1236−1244.
(10) Belpassi, L.; Reca, M. L.; Tarantelli, F.; Roncaratti, L. F.; Pirani, F.; Cappelletti, D.; Faure, A.; Scribano, Y. *J. Am. Chem. Soc.* **2010**, *132*, 13046−13058.
(11) Cappelletti, D.; Ronca, E.; Belpassi, L.; Tarantelli, F.; Pirani, F. *Acc. Chem. Res.* **2012**, *45*, 1571−1580.
(12) Bartocci, A.; Cappelletti, D.; Pirani, F.; Tarantelli, F.; Belpassi, L. *J. Phys. Chem. A* **2014**, *118*, 6440−6450.
(13) Khaliullin, R. Z.; Bell, A. T.; Head-Gordon, M. *J. Chem. Phys.* **2008**, *128*, 184112.
(14) Khaliullin, R. Z.; Bell, A. T.; Head-Gordon, M. *Chem. - Eur. J.* **2009**, *15*, 851−855.
(15) Riley, K. E.; Hobza, P. *WIREs Comput. Mol. Sci.* **2011**, *1*, 3−17.
(16) Hobza, P. *Acc. Chem. Res.* **2012**, *45*, 663−672.
(17) Burns, L. A.; Vázquez-Mayagoitia, A.; Sumpter, B. G.; Sherrill, C. D. *J. Chem. Phys.* **2011**, *134*, 084107.
(18) Burns, L. A.; Marshall, M. S.; Sherrill, C. D. *J. Chem. Phys.* **2014**, *141*, 234111.
(19) Lao, K. U.; Herbert, J. M. *J. Phys. Chem. A* **2015**, *119*, 235−253.
(20) Kitaura, K.; Morokuma, K. *Int. J. Quantum Chem.* **1976**, *10*, 325−340.
(21) Bagus, P. S.; Hermann, K.; Bauschlicher, C. W., Jr. *J. Chem. Phys.* **1984**, *80*, 4378−4386.
(22) Stevens, W. J.; Fink, W. H. *Chem. Phys. Lett.* **1987**, *139*, 15−22.
(23) Glendening, E. D.; Streitwieser, A. *J. Chem. Phys.* **1994**, *100*, 2900−2909.
(24) Glendening, E. D. *J. Phys. Chem. A* **2005**, *109*, 11936−11940.
(25) Chen, W.; Gordon, M. S. *J. Phys. Chem.* **1996**, *100*, 14316−14328.
(26) Mo, Y.; Gao, J.; Peyerimhoff, S. D. *J. Chem. Phys.* **2000**, *112*, 5530−5538.
(27) Mo, Y.; Bao, P.; Gao, J. *Phys. Chem. Chem. Phys.* **2011**, *13*, 6760−6775.
(28) Bickelhaupt, F. M.; Baerends, E. J. In *Reviews in Computational Chemistry*, Vol. *15*; Lipkowitz, K. B., Boyd, D. B., Eds.; Wiley-VCH: New York, 2000; pp 1−86, DOI: 10.1002/9780470125922.ch1.
(29) Khaliullin, R. Z.; Cobar, E. A.; Lochan, R. C.; Bell, A. T.; Head-Gordon, M. *J. Phys. Chem. A* **2007**, *111*, 8753−8765.
(30) Horn, P. R.; Mao, Y.; Head-Gordon, M. *J. Chem. Phys.* **2016**, *144*, 114107.
(31) Reinhardt, P.; Piquemal, J.-P.; Savin, A. *J. Chem. Theory Comput.* **2008**, *4*, 2020−2029.
(32) Su, P.; Li, H. *J. Chem. Phys.* **2009**, *131*, 014102.
(33) Mitoraj, M. P.; Michalak, A.; Ziegler, T. *J. Chem. Theory Comput.* **2009**, *5*, 962−975.
(34) Mandado, M.; Hermida-Ramón, J. M. *J. Chem. Theory Comput.* **2011**, *7*, 633−641.
(35) Yamada, K.; Koga, N. *Theor. Chem. Acc.* **2012**, *131*, 1178.
(36) von Hopffgarten, M.; Frenking, G. *WIREs Comput. Mol. Sci.* **2012**, *2*, 43−62.
(37) Phipps, M. J. S.; Fox, T.; Tautermann, C. S.; Skylaris, C.-K. *Chem. Soc. Rev.* **2015**, *44*, 3177−3211.
(38) Jeziorski, B.; Moszynski, R.; Szalewicz, K. *Chem. Rev.* **1994**, *94*, 1887−1930.
(39) Hohenstein, E. G.; Sherrill, C. D. *WIREs Comput. Mol. Sci.* **2012**, *2*, 304−326.
(40) Szalewicz, K. *WIREs Comput. Mol. Sci.* **2012**, *2*, 254−272.
(41) Jansen, G. *WIREs Comput. Mol. Sci.* **2014**, *4*, 127−144.
(42) van Duijneveldt, F. B.; van Duijneveldt-van de Rijdt, J. G. C. M.; van Lenthe, J. H. *Chem. Rev.* **1994**, *94*, 1873−1885.
(43) Tschumper, G. S. In *Reviews in Computational Chemistry*, Vol. *26*; Lipkowitz, K. B., Cundari, T. R., Eds.; Wiley: Hoboken, NJ, USA, 2009; Chapter 2, pp 39−90, DOI: 10.1002/9780470399545.ch2.
(44) Richard, R. M.; Lao, K. U.; Herbert, J. M. *J. Phys. Chem. Lett.* **2013**, *4*, 2674−2680.
(45) Szalewicz, K. *Acc. Chem. Res.* **2014**, *47*, 3266−3274.
(46) Schmidt, J. R.; Yu, K.; McDaniel, J. G. *Acc. Chem. Res.* **2015**, *48*, 548−556.
(47) Stone, A. J.; Misquitta, A. J. *Chem. Phys. Lett.* **2009**, *473*, 201−205.
(48) Azar, R. J.; Horn, P. R.; Sundstrom, E. J.; Head-Gordon, M. *J. Chem. Phys.* **2013**, *138*, 084102.
(49) Horn, P. R.; Sundstrom, E. J.; Baker, T. A.; Head-Gordon, M. *J. Chem. Phys.* **2013**, *138*, 134119.
(50) Kaduk, B.; Kowalczyk, T.; Van Voorhis, T. *Chem. Rev.* **2012**, *112*, 321−370.
(51) Wu, Q.; Ayers, P. W.; Zhang, Y. *J. Chem. Phys.* **2009**, *131*, 164112.
(52) Řezáč, J.; de la Lande, A. *J. Chem. Theory Comput.* **2015**, *11*, 528−537.
(53) Lao, K. U.; Herbert, J. M. Implementation of restricted and unrestricted versions of extended symmetry-adapted perturbation theory (XSAPT) in the atomic orbital basis, and benchmark calculations for large supramolecular complexes. Manuscript in preparation.
(54) Heßelmann, A. *J. Chem. Phys.* **2008**, *128*, 144112.
(55) Heßelmann, A. *J. Phys. Chem. A* **2011**, *115*, 11321−11330.
(56) Horn, P. R.; Head-Gordon, M. *J. Chem. Phys.* **2015**, *143*, 114111.
(57) Horn, P. R.; Head-Gordon, M. *J. Chem. Phys.* **2016**, *144*, 084118.
(58) Azar, R. J.; Head-Gordon, M. *J. Chem. Phys.* **2012**, *136*, 024103.
(59) Thirman, J.; Head-Gordon, M. *J. Chem. Phys.* **2015**, *143*, 084124.
(60) Khaliullin, R. Z.; Head-Gordon, M.; Bell, A. T. *J. Chem. Phys.* **2006**, *124*, 204105.
(61) Grimme, S. *WIREs Comput. Mol. Sci.* **2011**, *1*, 211−228.
(62) Grimme, S. *J. Comput. Chem.* **2004**, *25*, 1463−1473.
(63) Pernal, K.; Podeszwa, R.; Patkowski, K.; Szalewicz, K. *Phys. Rev. Lett.* **2009**, *103*, 263201.
(64) Lao, K. U.; Herbert, J. M. *J. Chem. Phys.* **2014**, *140*, 044108.
(65) Hapka, M.; Rajchel, L.; Modrzejewski, M.; Chałasiǹski, G.; Szczęśniak, M. M. *J. Chem. Phys.* **2014**, *141*, 134120.
(66) Moszynski, R.; Jeziorski, B.; Ratkiewicz, A.; Rybak, S. *J. Chem. Phys.* **1993**, *99*, 8856.
(67) Moszyński, R.; Cybulski, S. M.; Chałasiński, G. *J. Chem. Phys.* **1994**, *100*, 4998−5010.
(68) Herbert, J. M.; Jacobson, L. D.; Lao, K. U.; Rohrdanz, M. A. *Phys. Chem. Chem. Phys.* **2012**, *14*, 7679−7699.
(69) Lao, K. U.; Herbert, J. M. *J. Chem. Phys.* **2013**, *139*, 034107.
(70) Heßelmann, A.; Jansen, G.; Schütz, M. *J. Chem. Phys.* **2005**, *122*, 014103.
(71) Beer, M. Effiziente 'ab-initio' Berechnung molekularer Eigenschaften großer Systeme. Ph.D. thesis, University of Munich (LMU), 2011.
(72) Hapka, M.; Zuchowski, P. S.; Szczęśniak, M. M.; Chałasiǹski, G. *J. Chem. Phys.* **2012**, *137*, 164104.
(73) Lao, K. U.; Herbert, J. M. *J. Phys. Chem. Lett.* **2012**, *3*, 3241−3248.
(74) Grimme, S.; Antony, J.; Ehrlich, S.; Krieg, H. *J. Chem. Phys.* **2010**, *132*, 154104.
(75) Stone, A. J. *Chem. Phys. Lett.* **1993**, *211*, 101−109.
(76) Wu, Q.; Van Voorhis, T. *Phys. Rev. A: At., Mol., Opt. Phys.* **2005**, *72*, 024502.
(77) Wu, Q.; Van Voorhis, T. *J. Chem. Theory Comput.* **2006**, *2*, 765−774.
(78) Wu, Q.; Van Voorhis, T. *J. Chem. Phys.* **2006**, *125*, 164105.
(79) Ronca, E.; Belpassi, L.; Tarantelli, F. *ChemPhysChem* **2014**, *15*, 2682−2687.

DOI: 10.1021/acs.jctc.6b00155
J. Chem. Theory Comput. 2016, 12, 2569−2582

(80) Reed, A. E.; Curtiss, L. A.; Weinhold, F. *Chem. Rev.* **1988**, *88*, 899−926.
(81) Becke, A. D. *J. Chem. Phys.* **1988**, *88*, 2547−2553.
(82) Hirshfeld, F. L. *Theor. Chem. Acc.* **1977**, *44*, 129−138.
(83) Wu, Q.; Cheng, C.-L.; Van Voorhis, T. *J. Chem. Phys.* **2007**, *127*, 164119.
(84) Wu, Q.; Kaduk, B.; Van Voorhis, T. *J. Chem. Phys.* **2009**, *130*, 034109.
(85) Oberhofer, H.; Blumberger, J. *J. Chem. Phys.* **2009**, *131*, 064101.
(86) Becke, A. D. *J. Chem. Phys.* **1993**, *98*, 5648−5652.
(87) Lee, C.; Yang, W.; Parr, R. G. *Phys. Rev. B: Condens. Matter Mater. Phys.* **1988**, *37*, 785−789.
(88) Lin, Y.-S.; Li, G.-D.; Mao, S.-P.; Chai, J.-D. *J. Chem. Theory Comput.* **2013**, *9*, 263−272.
(89) Stoll, H.; Wagenblast, G.; Preuss, H. *Theor. Chem. Acc.* **1980**, *57*, 169−178.
(90) Rohrdanz, M. A.; Martins, K. M.; Herbert, J. M. *J. Chem. Phys.* **2009**, *130*, 054112.
(91) Lange, A. W.; Herbert, J. M. *J. Am. Chem. Soc.* **2009**, *131*, 3913−3922.
(92) Modrzejewski, M.; Rajchel, L.; Chalasinski, G.; Szczesniak, M. M. *J. Phys. Chem. A* **2013**, *117*, 11580−11586.
(93) Shao, Y.; Gan, Z.; Epifanovsky, E.; Gilbert, A. T. B.; Wormit, M.; Kussmann, J.; Lange, A. W.; Behn, A.; Deng, J.; Feng, X.; Ghosh, D.; Goldey, M.; Horn, P. R.; Jacobson, L. D.; Kaliman, I.; Khaliullin, R. Z.; Kús, T.; Landau, A.; Liu, J.; Proynov, E. I.; Rhee, Y. M.; Richard, R. M.; Rohrdanz, M. A.; Steele, R. P.; Sundstrom, E. J.; Woodcock, H. L., III; Zimmerman, P. M.; Zuev, D.; Albrecht, B.; Alguire, E.; Austin, B.; Beran, G. J. O.; Bernard, Y. A.; Berquist, E.; Brandhorst, K.; Bravaya, K. B.; Brown, S. T.; Casanova, D.; Chang, C.-M.; Chen, Y.; Chien, S. H.; Closser, K. D.; Crittenden, D. L.; Diedenhofen, M.; DiStasio, R. A., Jr.; Do, H.; Dutoi, A. D.; Edgar, R. G.; Fatehi, S.; Fusti-Molnar, L.; Ghysels, A.; Golubeva-Zadorozhnaya, A.; Gomes, J.; Hanson-Heine, M. W. D.; Harbach, P. H. P.; Hauser, A. W.; Hohenstein, E. G.; Holden, Z. C.; Jagau, T.-C.; Ji, H.; Kaduk, B.; Khistyaev, K.; Kim, J.; Kim, J.; King, R. A.; Klunzinger, P.; Kosenkov, D.; Kowalczyk, T.; Krauter, C. M.; Lao, K. U.; Laurent, A.; Lawler, K. V.; Levchenko, S. V.; Lin, C. Y.; Liu, F.; Livshits, E.; Lochan, R. C.; Luenser, A.; Manohar, P.; Manzer, S. F.; Mao, S.-P.; Mardirossian, N.; Marenich, A. V.; Maurer, S. A.; Mayhall, N. J.; Neuscamman, E.; Oana, C. M.; Olivares-Amaya, R.; O'Neill, D. P.; Parkhill, J. A.; Perrine, T. M.; Peverati, R.; Pieniazek, P. A.; Prociuk, A.; Rehn, D. R.; Rosta, E.; Russ, N. J.; Sharada, S. M.; Sharma, S.; Small, D. W.; Sodt, A.; Stein, T.; Stück, D.; Su, Y.-C.; Thom, A. J. W.; Tsuchimochi, T.; Vanovschi, V.; Vogt, L.; Vydrov, O.; Wang, T.; Watson, M. A.; Wenzel, J.; White, A.; Williams, C. F.; Yang, J.; Yeganeh, S.; Yost, S. R.; You, Z.-Q.; Zhang, I. Y.; Zhang, X.; Zhao, Y.; Brooks, B. R.; Chan, G. K. L.; Chipman, D. M.; Cramer, C. J.; Goddard, W. A., III; Gordon, M. S.; Hehre, W. J.; Klamt, A.; Schaefer, H. F., III; Schmidt, M. W.; Sherrill, C. D.; Truhlar, D. G.; Warshel, A.; Xu, X.; Aspuru-Guzik, A.; Baer, R.; Bell, A. T.; Besley, N. A.; Chai, J.-D.; Dreuw, A.; Dunietz, B. D.; Furlani, T. R.; Gwaltney, S. R.; Hsu, C.-P.; Jung, Y.; Kong, J.; Lambrecht, D. S.; Liang, W.; Ochsenfeld, C.; Rassolov, V. A.; Slipchenko, L. V.; Subotnik, J. E.; Van Voorhis, T.; Herbert, J. M.; Krylov, A. I.; Gill, P. M. W.; Head-Gordon, M. *Mol. Phys.* **2015**, *113*, 184−215.
(94) Cobar, E. A.; Horn, P. R.; Bergman, R. G.; Head-Gordon, M. *Phys. Chem. Chem. Phys.* **2012**, *14*, 15328−15339.
(95) Reed, A. E.; Weinstock, R. B.; Weinhold, F. *J. Chem. Phys.* **1985**, *83*, 735−746.
(96) Karthikeyan, S.; Sedlak, R.; Hobza, P. *J. Phys. Chem. A* **2011**, *115*, 9422−9428.
(97) Hammerum, S.; Nielsen, C. B. *J. Phys. Chem. A* **2005**, *109*, 12046−12053.
(98) Cohen, A. J.; Mori-Sanchez, P.; Yang, W. *Science* **2008**, *321*, 792−794.
(99) Cohen, A. J.; Mori-Sanchez, P.; Yang, W. *Chem. Rev.* **2012**, *112*, 289−320.
(100) Steinmann, S. N.; Piemontesi, C.; Delachat, A.; Corminboeuf, C. *J. Chem. Theory Comput.* **2012**, *8*, 1629−1640.
(101) Johnson, E. R.; Salamone, M.; Bietti, M.; DiLabio, G. A. *J. Phys. Chem. A* **2013**, *117*, 947−952.
(102) Barnett, R. N.; Bongiorno, A.; Cleveland, C. L.; Joy, A.; Landman, U.; Schuster, G. B. *J. Am. Chem. Soc.* **2006**, *128*, 10795−10800.
(103) Cadet, J.; Douki, T.; Ravanat, J.-L. *Acc. Chem. Res.* **2008**, *41*, 1075−1083.
(104) Mizuse, K.; Hasegawa, H.; Mikami, N.; Fujii, A. *J. Phys. Chem. A* **2010**, *114*, 11060−11069.
(105) Lias, S. G.; Bartmess, J. E.; Liebman, J. F.; Holmes, J. L.; Levin, R. D.; Mallard, W. G. Ion Energetics Data. *NIST Chemistry WebBook*, NIST Standard Reference Database No. 69; National Institute of Standards and Technology: Gaithersburg, MD, USA, 2011.
(106) Becke, A. D.; Johnson, E. R. *J. Chem. Phys.* **2005**, *122*, 154104.
(107) Becke, A. D.; Johnson, E. R. *J. Chem. Phys.* **2005**, *123*, 154101.
(108) Attah, I. K.; Platt, S. P.; Meot-Ner, M.; El-Shall, M. S.; Peverati, R.; Head-Gordon, M. *J. Phys. Chem. Lett.* **2015**, *6*, 1111−1118.
(109) Badger, B.; Brocklehurst, B. *Nature* **1968**, *219*, 263.
(110) Kobayashi, H.; Tomita, H.; Naito, T.; Kobayashi, A.; Sakai, F.; Watanabe, T.; Cassoux, P. *J. Am. Chem. Soc.* **1996**, *118*, 368−377.
(111) Kochi, J. K.; Rathore, R.; Magueres, P. L. *J. Org. Chem.* **2000**, *65*, 6826−6836.
(112) Meot-Ner, M. *J. Phys. Chem.* **1980**, *84*, 2724−2728.
(113) Peverati, R.; Truhlar, D. G. *J. Phys. Chem. Lett.* **2011**, *2*, 2810−2817.
(114) Hohenstein, E. G. *Implementation and Applications of Density-Fitted Symmetry-Adapted Perturbation Theory*. Ph.D. thesis, Georgia Institute of Technology, 2011.
(115) Jaeger, H. M.; Schaefer, H. F.; Hohenstein, E. G.; Sherrill, C. D. *Comput. Theor. Chem.* **2011**, *973*, 47−52.
(116) Ohio Supercomputer Center, http://osc.edu/ark:/19495/f5s1ph73.

NOTE ADDED AFTER ASAP PUBLICATION

Notation error $C_6H_5^{\bullet+}$ was corrected to $C_6H_6^{\bullet+}$ in sections IVG and IVH, and no data or conclusions were affected; the correct version reposted May 27, 2016.

DOI: 10.1021/acs.jctc.6b00155
J. Chem. Theory Comput. 2016, 12, 2569−2582